2015-06-12

Multi-mode Flight Sliding Mode Control System for a Quadrotor

Villanueva, Abraham; Castillo-Toledo, Bernardino; Bayro-Corrochano, Eduardo; Luque-Vega, Luis F.; González-Jiménez, Luis E.

Villanueva, A.; Castillo-Toledo, B.; Bayro-Corrochano, E.;Luque-Vega, L.F., and González-Jiménez, L.E. (2015). Multi-mode Flight Sliding Mode Control System for a Quadrotor. 2015 International Conference on Unmanned Aircraft Systems.

2015 International Conference on Unmanned Aircraft Systems (ICUAS)
Denver Marriott Tech Center
Denver, Colorado, USA, June 9-12, 2015

Multi-mode Flight Sliding Mode Control System for a Quadrotor

Abraham Villanueva, B. Castillo-Toledo and Eduardo Bayro-Corrochano

Department of Automatic Control
CINVESTAV-IPN Unidad Guadalajara
Zapopan, Jalisco, Mexico
Email: oavillanueva@gdl.cinvestav.mx
Email: toledo@gdl.cinvestav.mx
Email: edb@gdl.cinvestav.mx

Luis F. Luque-Vega and Luis E. González-Jiménez

Department of Electronics, Systems and Informatics. ITESO University
Tlaquepaque, Jalisco, Mexico
Email: luisluque@iteso.mx
Email: luisgonzalez@iteso.mx

***Abstract*—There is a wide range of applications for unmanned aerial vehicles that requires the capability of having several and robust flight controllers available. This paper presents the main framework of a multi-mode flight control system for a quadrotor based on the super twisting control algorithm. The design stages for the four flight control modes encompassing manual, altitude, GPS fixed and autonomous mode are presented. The stability proof for each flight mode is carried out by means of Lyapunov functions while the stability analysis for the complete system, when a transition from one mode to another occurs, is demonstrated using the switching nonlinear systems theory. The performance of the proposed framework is demonstrated in a simulation study taking into account external disturbances.**

Keywords–Multi-mode flight control; Sliding modes; Quadrotor.

I. INTRODUCTION

The Unmanned Aerial Vehicles (UAVs), especially multi-rotors, are becoming the mainstream in civilian realm for performing a wide range of applications involving detection, recognition and identification of different objects of interest. This is due to the advantages that this kind of aircrafts presents in comparison to others like vertical take-off and landing, hovering, the ability to follow a sharp trajectory, among others.

One of the most popular multirotor today is the quadrotor. This multirotor is highly nonlinear, under-actuated and subject to disturbances and parameter uncertainties. Most of the research carried out on this platform have tackled the stabilization and the trajectory tracking problem. There are several interesting robust flight controllers proposed for solving the stabilization problem, e.g., super twisting control algorithm [1], fuzzy control [2], a backstepping approach taking into account the actuator faults [3], among others. Moreover, for the trajectory tracking problem, a feedback linearization controller with a high order sliding mode observer [4], a backstepping control with a sliding mode observer [5], a combination of backstepping and sliding mode control [6], have been applied with satisfactory results.

All the aforementioned flight controllers focused in one single flight mode; therefore, it represents a great challenge to design a multi-mode flight control system. There are a wide range of applications for multi-rotors that require the capability of having several and robust flight controllers available such as forest fire detection, power line inspection, surveillance, etc. This paper presents the main framework of a multi-mode flight control system for a quadrotor based on the super twisting control algorithm, taking into account four different flight modes: manual, altitude, GPS fixed and autonomous mode.

The paper is organized as follows: in the following section, the description of the quadrotor dynamics is described. The design stages for the complete multi-mode flight framework are presented in Section III. Then, Section IV presents the stability analysis for each flight mode and for

978-1-4799-6009-5/15/$31.00 ©2015 IEEE

the complete system in the event of a transition from one flight mode to another. Simulation results illustrating the effectiveness of the proposed framework in presence of external disturbances are given in Section V and some conclusions close the paper.

II. Quadrotor Dynamics

The dynamic model is derived under the following assumptions: the structure is supposed to be rigid and symmetrical, the center of mass and the body fixed frame origin are assumed to coincide, and the propellers are supposed rigid.

The equations describing the attitude and position of a quadrotor helicopter are basically those of a rotating rigid body with six degrees of freedom (DoF) [7]. Let us consider two main reference frames: the earth fixed frame E^E and body fixed frame E^B which is fixed at the center of mass of the quadrotor.

The space orientation of the aircraft between E^B and E^E is given by the transformation velocity matrix $R(\Theta)$ and the rotation velocity matrix $M(\Theta)$ [8]. These matrices are given by[1]

$$R(\Theta) = \begin{bmatrix} C_\psi C_\theta & C_\psi S_\theta S_\phi - S_\psi C_\phi & C_\psi S_\theta C_\phi + S_\psi S_\phi \\ S_\psi C_\theta & S_\psi S_\theta S_\phi + C_\psi C_\phi & S_\psi S_\theta C_\phi - C_\psi S_\phi \\ -S_\theta & C_\theta S_\phi & C_\theta C_\phi \end{bmatrix} \quad (1)$$

and

$$M(\Theta) = \begin{bmatrix} 1 & 0 & -S_\theta \\ 0 & C_\phi & C_\theta S_\phi \\ 0 & -S_\phi & C_\theta C_\phi \end{bmatrix}. \quad (2)$$

The dynamic model is derived using Newton-Euler formalism in the body fixed frame E^B, about the rotorcraft subjected to external forces ΣF_{ext} and moments ΣT_{ext} applied to the center of mass. Thus, the dynamic equations of motion are described by

$$\begin{array}{rcl} \Sigma F_{ext} & = & m\dot{V_B} + \Omega \times mV_B \\ \Sigma T_{ext} & = & I\dot{\Omega} + \Omega \times I\Omega \end{array} \quad (3)$$

where m is the mass of the quadrotor, $I = diag(I_x, I_y, I_z)$ the inertia matrix of the helicopter, V_B the linear translational velocity and Ω the angular velocity. The external forces and moments are expressed in the body-fixed frame as

$$\begin{array}{rcl} \Sigma F_{ext} & = & F_{prop} - F_{aero} - F_{grav} \\ \Sigma T_{ext} & = & T_{prop} - T_{aero} - T_{gyro} \end{array} \quad (4)$$

where $F_{prop} = col(0, 0, U_1)$ is the forces vector and $T_{prop} = col(U_2, U_3, U_4)$ the moments vector produced by the propellers. $F_{grav} = mR(\Theta)^T G$ is the gravity effect force with $G = col(0, 0, 9.81) m/s^2$, $F_{aero} = col(A_x, A_y, A_z)$ and $T_{aero} = col(A_p, A_q, A_r)$ are the aerodynamic forces and moments acting on the UAV, respectively. $T_{gyro} = \sum_{i=1}^{4} J(\Omega \times e_3)(-1)^{i+1}\omega_i$ defines the gyroscopic effects resulting from the propeller rotations. The inputs $U_i (i = 1, 2, 3, 4)$ are defined as

$$\begin{array}{l} U_1 = \sum_{i=1}^{4} F_i \\ U_2 = d(F_4 - F_2) \\ U_3 = d(F_3 - F_1) \\ U_4 = c\sum_{i=1}^{4}(-1)^i F_i \end{array} \quad (5)$$

where d is the distance from the center of mass to the rotor shaft, c is the drag factor, J is the rotor inertia, and $F_i = bw_i^2, (i = 1, 2, 3, 4)$ is the force generated by the rotational speed of the motor ω_i and the thrust factor b. The aerodynamic functions A_i are computed as $A_i = \frac{1}{2}\rho C_i W^2$ from the aerodynamic coefficients C_i, the air density ρ, and $W = \Omega - \Omega_{air}$ which is the velocity of the aircraft with respect to the air. Using (3) and (4) the equations describing the dynamics of the quadcopter can be expressed in the reference frame E_E as

$$\ddot{X}_E = \frac{1}{m}R(\Theta)[F_{prop} - F_{aero}] - G$$

$$\ddot{\Theta} = [IM(\Theta)]^{-1} \begin{bmatrix} T_{prop} - T_{aero} - T_{gyro} - M(\Theta)\dot{\Theta}\times \\ IM(\Theta)\dot{\Theta} - I\left(\frac{\partial M(\Theta)}{\partial \theta}\dot{\theta} + \frac{\partial M(\Theta)}{\partial \phi}\dot{\phi}\right)\dot{\Theta} \end{bmatrix} \quad (6)$$

and simplifying the matrix $M(\Theta)$ as the identity due to small variations of the attitude angles of the

[1]The abbreviations $S_{(\cdot)}$ and $C_{(\cdot)}$ denote $\sin(\cdot)$ and $\cos(\cdot)$, respectively.

aircraft, we can express the following equations

$$\begin{aligned}
\ddot{x} &= \tfrac{U_1}{m}\left(S_\phi S_\psi + C_\phi S_\theta C_\psi\right) - A_x \\
\ddot{y} &= \tfrac{U_1}{m}\left(-S_\phi C_\psi + C_\phi S_\theta S_\psi\right) - A_y \\
\ddot{z} &= \tfrac{U_1}{m}\left(C_\phi C_\theta\right) - g - A_z \\
\ddot{\phi} &= \tfrac{1}{I_x}\left(U_2 + \left(I_y - I_z\right)\dot{\theta}\dot{\psi} + J\dot{\theta}\omega\right) - A_p \\
\ddot{\theta} &= \tfrac{1}{I_y}\left(U_3 + \left(I_z - I_x\right)\dot{\phi}\dot{\psi} + J\dot{\phi}\omega\right) - A_q \\
\ddot{\psi} &= \tfrac{1}{I_z}\left(U_4 + \left(I_x - I_y\right)\dot{\phi}\dot{\theta}\omega\right) - A_r.
\end{aligned} \tag{7}$$

Then, writing the system in the state space form, assigning $X = [x, \dot{x}, y, \dot{y}, z, \dot{z}, \phi, \dot{\phi}, \theta, \dot{\theta}, \psi, \dot{\psi},]^T$, we obtain the following state-space representation

$$\begin{aligned}
\dot{x}_1 &= x_2 \\
\dot{x}_2 &= \tfrac{U_1}{m}\left(S_{x_7} S_{x_{11}} + C_{x_7} S_{x_9} C_{x_{11}}\right) - A_2 \\
\dot{x}_3 &= x_4 \\
\dot{x}_4 &= \tfrac{U_1}{m}\left(-S_{x_7} C_{x_{11}} + C_{x_7} S_{x_9} S_{x_{11}}\right) - A_4 \\
\dot{x}_5 &= x_6 \\
\dot{x}_6 &= \tfrac{U_1}{m}\left(C_{x_7} C_{x_9}\right) - g - A_6 \\
\dot{x}_7 &= x_8 \\
\dot{x}_8 &= \tfrac{1}{I_x}\left(U_2 + \left(I_y - I_z\right) x_{10} x_{12} + J x_{10}\omega\right) - A_8 \\
\dot{x}_9 &= x_{10} \\
\dot{x}_{10} &= \tfrac{1}{I_y}\left(U_3 + \left(I_z - I_x\right) x_8 x_{12} + J x_8 \omega\right) - A_{10} \\
\dot{x}_{11} &= x_{12} \\
\dot{x}_{12} &= \tfrac{1}{I_z}\left(U_4 + \left(I_x - I_y\right) x_8 x_{10}\right) - A_{12}
\end{aligned} \tag{8}$$

with $X = [x_1, x_2, ..., x_{12}]^T$.

III. Multi-mode Flight Control Design

The multi-mode flight control system considered for the quadrotor must provide four different flight modes: manual, altitude, GPS fixed and autonomous mode. The four flight modes have a similar control structure, their main differences are the references that are required for each flight mode and its corresponding outputs. The four flight modes share the same control law for roll and pitch angles; this fact will be helpful when stability analysis is presented in next section. The description of each flight mode and its common applications is given below.

A. Manual Control Mode

Manual control mode allows the pilot to fly the quadrotor manually, controlling the roll, pitch and yaw angles. The RC remote controller is used to drive the quadrotor to the desire x and y position through regularly roll and pitch commands in order to withstand the wind effects. The throttle stick controls the z position of the quadrotor, for heading control if the pilot releases the yaw stick the quadrotor will maintain its current heading.

This flight mode is the standard for almost all the quadrotors in the market, because of its intuitive manner to fly the vehicle. Almost all applications need this flight mode in order to have full control on the displacements of the vehicle but it has its main application in aerial filming. However, the pilot requires several hours of training to master this flight mode due to the zero dynamics in the xy plane.

The control objective for manual flight control is to ensure the asymptotic convergence of the variables (x_7, x_9, x_{11}) to the references $(x_{7r}, x_{9r}, x_{11r})$ in (8) by means of U_2, U_3 and U_4.

1) Roll Angle Dynamics: Defining the tracking error for roll angles and taken its derivative, we yield to

$$\begin{aligned}
z_7 &= x_{7r} - x_7 \\
\dot{z}_7 &= \dot{x}_{7r} - x_8 \\
\ddot{z}_7 &= \ddot{x}_{7r} - \tfrac{1}{I_x}\left(U_2 + \left(I_y - I_z\right) x_{10} x_{12} + J x_{10}\omega\right) + A_8.
\end{aligned} \tag{9}$$

Then, we define the sliding mode surface as

$$\begin{aligned}
\sigma_7 &= \dot{z}_7 + k_7 z_7 \\
\dot{\sigma}_7 &= \overline{f}_7 - V_7
\end{aligned} \tag{10}$$

with $\overline{f}_7 = \ddot{x}_{7r} - \frac{1}{I_x}\left(\left(I_y - I_z\right) x_{10} x_{12} + J x_{10}\omega\right) + A_8 + k_7 \dot{z}_7$, $V_7 = \frac{1}{I_x} U_2$, and $k_7 > 0$.

2) Pitch Angle Dynamics: Define the tracking error for pitch angle

$$\begin{aligned}
z_9 &= x_{9r} - x_9 \\
\dot{z}_9 &= \dot{x}_{9r} - x_{10} \\
\ddot{z}_9 &= \ddot{x}_{9r} - \tfrac{1}{I_y}\left(U_3 + \left(I_z - I_x\right) x_8 x_{12} + J x_8 \omega\right) + A_{10}
\end{aligned} \tag{11}$$

and define the sliding mode surface as

$$\begin{aligned}
\sigma_9 &= \dot{z}_9 + k_9 z_9 \\
\dot{\sigma}_9 &= \overline{f}_9 - V_9
\end{aligned} \tag{12}$$

with $\overline{f}_9 = \ddot{x}_{9r} - \frac{1}{I_y}\left(\left(I_z - I_x\right) x_8 x_{12} + J x_8 \omega\right) + A_{10} + k_9 \dot{z}_9$, $V_9 = \frac{1}{I_y} U_3$, and $k_9 > 0$.

3) Yaw Angle Dynamics: Define the tracking error for yaw angle as

$$\begin{aligned} z_{11} &= x_{11r} - x_{11} \\ \dot{z}_{11} &= \dot{x}_{11r} - x_{12} \\ \ddot{z}_{11} &= \ddot{x}_{11r} - \frac{1}{I_z}\left(U_4 + \left(I_x - I_y\right) x_8 x_{10}\right) + A_{12} \end{aligned} \tag{13}$$

and define the sliding mode surface as

$$\begin{aligned} \sigma_{11} &= \dot{z}_{11} + k_{11} z_{11} \\ \dot{\sigma}_{11} &= \overline{f}_{11} - V_{11} \end{aligned} \tag{14}$$

with $\overline{f}_{11} = \ddot{x}_{11r} - \frac{1}{I_z}\left(U_4 + \left(I_x - I_y\right) x_8 x_{10}\right) + A_{12} + k_{11}\dot{z}_{11}$, $V_{11} = \frac{1}{I_z} U_4$, and $k_{11} > 0$.

In order to make the sliding surface converge to zero, we applied the super twisting control algorithm in the Euler angles.

4) Sliding Mode Control Design for Manual Control: From (10), (12) and (14), the projection motion in the subspaces σ_7, σ_9 and σ_{11} is described by

$$\begin{bmatrix} \dot{\sigma}_7 \\ \dot{\sigma}_9 \\ \dot{\sigma}_{11} \end{bmatrix} = \begin{bmatrix} \overline{f}_7 \\ \overline{f}_9 \\ \overline{f}_{11} \end{bmatrix} - \begin{bmatrix} V_7 \\ V_9 \\ V_{11} \end{bmatrix} \tag{15}$$

where

$$\begin{bmatrix} V_7 \\ V_9 \\ V_{11} \end{bmatrix} = B \begin{bmatrix} U_2 \\ U_3 \\ U_4 \end{bmatrix}, \quad B = \begin{bmatrix} \frac{1}{I_x} & 0 & 0 \\ 0 & \frac{1}{I_y} & 0 \\ 0 & 0 & \frac{1}{I_z} \end{bmatrix}. \tag{16}$$

Now, we design the control inputs applying the super twisting control algorithm [9]:

$$\begin{aligned} &V_i = \lambda_i \left|\sigma_i\right|^{1/2} sign(\sigma_i) + \sigma_{i+1}, \quad i = 7, 9, 11, \\ &\dot{\sigma}_{i+1} = \alpha_i sign(\sigma_i) \end{aligned} \tag{17}$$

with control gains $\lambda_i > 0$ and $\alpha_i > 0$.

These super twisting controllers ensure the asymptotic tracking of $(x_{7r}, x_{9r}, x_{11r})$, but we need to define the form of U_1 as

$$U_1 = \frac{Th_r + m\left(g + Az\right)}{C_{x7} C_{x9}} \tag{18}$$

where Th_r is a throttle reference based on the limits of the thrust force that can be generated by the four motors and the limits of the RC throttle stick lever.

B. Altitude Control Mode

In altitude control mode the quadrotor maintains a fixed altitude while roll, pitch, and yaw are available to be manually controlled. In this mode the variables to control are altitude (z position), roll, pitch and yaw angles. A barometer, GPS or laser is needed in order to know the current altitude of the aircraft. In this case, we consider a GPS sensor in which the reference for the absolute position of the quadrotor is generated in a global reference frame. A transformation from this global frame to a local reference frame is carried out in order to handle local trajectories for the absolute position of the quadrotor. This flight mode overcomes the issue of losing thrust force on throttle when displacing along other directions. The most common applications for this flight mode are all the tasks that require inspection of large area like agriculture, lakes, protected areas, etc., since the pilot does not have to worry about the altitude of the aircraft while we can move along the xy plane.

The control objective is to drive the variables (x_5, x_7, x_9, x_{11}) to the reference vector $(x_{5r}, x_{7r}, x_{9r}, x_{11r})$. It can be noted that the controllers for roll, pitch and yaw angles are the same as in the manual mode, and are described by (17), therefore just the procedure for z position controller must be defined.

1) z Position Dynamics: Let us define the tracking error for the altitude position and its dynamics as

$$\begin{aligned} z_5 &= x_{5r} - x_5 \\ \dot{z}_5 &= \dot{x}_{5r} - x_6 \\ \ddot{z}_5 &= \ddot{x}_{5r} - \frac{U_1}{m}\left(C_{x_7} C_{x_9}\right) + g + A_6 \end{aligned} \tag{19}$$

and design the sliding mode surface as

$$\begin{aligned} \sigma_5 &= \dot{z}_5 + k_5 z_5 \\ \dot{\sigma}_5 &= \overline{f}_5 - V_5 \end{aligned} \tag{20}$$

with $\overline{f}_5 = \ddot{x}_{5r} + g + A_6 + k_5 \dot{z}_5$, $V_5 = \frac{C_{x_7} C_{x_9}}{m} U_1$, and $k_5 > 0$.

Since the selection of U_1 will allow us to design a smooth sliding manifolds for the x and y displacements, for the other two flight modes we

apply the super twisting control algorithm with a sigmoid function as follows

$$\begin{aligned} V_5 &= \lambda_5 \left|\sigma_5\right|^{1/2} sigm(\varepsilon_5, \sigma_5) + \sigma_6 \\ \dot{\sigma}_6 &= \alpha_5 sign(\sigma_5) \end{aligned} \tag{21}$$

with control gains $\lambda_5 > 0$ and $\alpha_5 > 0$. The sigmoid function used in this work is defined as

$$sigm(\varepsilon, \sigma) = tanh(\varepsilon\sigma). \tag{22}$$

C. GPS Fixed Mode

The GPS fixed mode automatically maintains the current location (longitude, latitude and altitude) and the heading of the quadrotor. The pilot may change the orientation about the yaw axis via the RC remote control.

This flight mode is useful for applications like search and rescue and fire detection tasks because the pilot can command, through the RC remote control, the quadrotor to hold its current position when it detects an object of interest.

The control objective is to drive the variables (x_1, x_3, x_5, x_{11}) to the reference vector $(x_{1r}, x_{3r}, x_{5r}, x_{11r})$. It can be noted that the controllers for roll, pitch, yaw angles and z position are the same as in the manual and altitude control mode, and are described by (17) and (20). Therefore just the longitude (x position) and latitude (y position) controllers have to be designed.

1) x Position Dynamics: To follow a desired longitudinal position we define the tracking error and its dynamics as

$$\begin{aligned} z_1 &= x_{1r} - x_1 \\ \dot{z}_1 &= \dot{x}_{1r} - x_2 \\ \ddot{z}_1 &= \ddot{x}_{1r} - \tfrac{U_1}{m}\left(S_{x_7} S_{x_{11}} + C_{x_7} S_{x_9} C_{x_{11}}\right) + A_2 \end{aligned} \tag{23}$$

Applying the block control technique we define the pseudo control $U_x = S_{x_7} S_{x_{11}} + C_{x_7} S_{x_9} C_{x_{11}}$, because the input U_1 has been already assigned to the dynamics of z position, this means that there exists a relation between the roll, pitch and yaw angles. Moreover, the translations in x and y directions depended on these angles. Then, we can define the sliding mode surface as

$$\begin{aligned} \sigma_1 &= \dot{z}_1 + k_1 z_1 \\ \dot{\sigma}_1 &= \overline{f}_1 - V_1 \end{aligned} \tag{24}$$

with $\overline{f}_1 = \ddot{x}_{1r} + A_2 + k_1 \dot{z}_1$, $V_1 = -\frac{U_1}{m} U_x$, and $k_1 > 0$.

2) y Position Dynamics: To follow a desired latitudinal position we define the tracking error and its dynamics as

$$\begin{aligned} z_3 &= x_{3r} - x_3 \\ \dot{z}_3 &= \dot{x}_{3r} - x_4 \\ \ddot{z}_1 &= \ddot{x}_{1r} - \tfrac{U_1}{m}\left(-S_{x_7} C_{x_{11}} + C_{x_7} S_{x_9} S_{x_{11}}\right) + A_4 \end{aligned} \tag{25}$$

Lets define the pseudo control $U_y = -S_{x_7} C_{x_{11}} + C_{x_7} S_{x_9} S_{x_{11}}$, and propose the next sliding mode surface

$$\begin{aligned} \sigma_3 &= \dot{z}_3 + k_3 z_3 \\ \dot{\sigma}_3 &= \overline{f}_3 - V_3 \end{aligned} \tag{26}$$

with $\overline{f}_3 = \ddot{x}_{3r} + A_y + k_3 \dot{z}_3$, $V_3 = -\frac{U_1}{m} U_y$, and $k_3 > 0$.

3) Sliding Mode Control Design for GPF Fixed Mode: Now, we can apply the super twisting control algorithm with the sigmoid function as in (21)

$$\begin{aligned} V_i &= \lambda_i \left|\sigma_i\right|^{1/2} sigm(\varepsilon_i, \sigma_i) + \sigma_{i+1}, \quad i = 1, 3, \\ \dot{\sigma}_{i+1} &= \alpha_i sign(\sigma_i) \end{aligned} \tag{27}$$

with control gains $\lambda_i > 0$ and $\alpha_i > 0$.

So far, we have generated a smooth form of the pseudo controls U_x and U_y. On the other hand, the references in x and y position will give us the desired U_x and U_y, then

$$\begin{aligned} U_{xd} &= S_{x_{7d}} S_{x_{11}} + C_{x_{7d}} S_{x_{9d}} C_{x_{11}} \\ U_{yd} &= -S_{x_{7d}} C_{x_{11}} + C_{x_{7d}} S_{x_{9d}} S_{x_{11}} \end{aligned} \tag{28}$$

Therefore, the problem of following desired x and y position is reduced to follow desired roll and pitch angles, which can be achieved by the laws of control defined in (17). But first we have to decouple x_{7d} and x_{9d} from the linear combination which is non singular for all x_{11}, and the solution for x_{7d} and x_{9d} is contained in $(-\pi/2, \pi/2)$, therefore

$$\begin{aligned} x_{7d} &= \arcsin(U_{xd} S_{x_{11}} + U_{yd} C_{x_{11}}) \\ x_{9d} &= \arcsin\left(\tfrac{U_{xd} C_{x_{11}} - U_{yd} S_{x_{11}}}{C(x_{7d})}\right) \end{aligned} \tag{29}$$

Now, we assign $x_{7r} = x_{7d}$ and $x_{9r} = x_{9d}$, and use the equations in (17) for achieving the convergence of these angles.

D. Autonomous Control Mode

In autonomous control mode the quadrotor will use pre-defined way-points to follow a desired trajectory. This is done via a ground station, while the RC remote control is used to activate the mission. The applications that can be fulfilled with this flight mode are drone-based delivery system, ambulance drone, surveillance, among others.

The objective control variables are the same than in the GPS fixed mode $(x_{1r}, x_{3r}, x_{5r}, x_{11r})$ but the main difference is that the references are generated from a user via a ground station or autonomously from path planning algorithm. The only assumption is that the generated trajectories must be smooth functions of time at least of class C^2.

IV. Closed Loop Stability

In this section the stability analysis of the proposed multi-mode flight framework is developed. First, we will state the stability proof for the complete system, without taking into account the transition from one flight mode to another. This will be carried out later.

A. Sliding Mode Stability

In order to establish the sliding mode stability condition for the Euler angles, we rewrite (15) with (17) as

$$\begin{aligned} \dot{s}_i &= \overline{f}_i - \lambda_i |s_i|^{1/2} sign(s_i) + s_{i+1}, \qquad i = 7, 9, 11, \\ \dot{s}_{i+1} &= \alpha_i sign(s_i). \end{aligned} \tag{30}$$

Now, we introduce the following assumption:

Assumption 1. *The perturbation term $\bar{f}_i$ is bounded in an admissible operation region D_1 by*

$$|f_i| \leq \delta_i |s_i|^{1/2}, \qquad i = 1, 3, 5, 7, 9, 11, \tag{31}$$

with constants $\delta_i > 0$.

Then, we can state the following theorem which assures the robustness of the convergence of the trajectory error to zero in finite time.

Theorem 1. *[10] Under assumption 1 the origin $s_i = 0$ is a locally asymptotically stable equilibrium point if the controller gains λ_i and α_i satisfy*

$$\begin{aligned} \lambda_i &> 2\bar{f}_i \\ \alpha_i &> \lambda_i \frac{5\bar{f}_i\lambda_i + 4\bar{f}_i^2}{2\left(\lambda_i - 2\bar{f}_i\right)}. \end{aligned} \tag{32}$$

Moreover, all trajectories converge to the origin in finite time, upperbounded by $T = \frac{2V_i^{1/2}(s_{i_0})}{\gamma_i}$, where s_{i_0} is the initial state and γ_i is a constant depending on the controller gains and the perturbation term.

Then, we use (21), and rewrite (27) with (24)-(24) in order to establish the sliding mode stability condition for the x, y and z positions, but first we introduce the following assumptions:

Assumption 2. *The sign function can be approximated by the sigmoid function as shown by the following limit:*

$$\lim_{\varepsilon \to \infty} sigm(\varepsilon_i, \sigma_i) = sign(\sigma_i) \tag{33}$$

Assumption 3. *Let us define the difference between sign and sigmoid function for a given ε is*

$$\Delta(\varepsilon_i, \sigma_i) = sign(\sigma_i) - sigm(\varepsilon_i, \sigma_i) \tag{34}$$

and $\Delta(\varepsilon_i, \sigma_i)$ is bounded i.e. there exists a positive constant ϱ such that

$$\|\Delta(\varepsilon_i, \sigma_i)\| \leq \varrho_i \leq 1 \tag{35}$$

Theorem 2. *[11] Under assumption 1 the origin $s_i = 0$ is a locally asymptotically stable equilibrium point if the controller gains λ_i and α_i satisfy*

$$\begin{aligned} \lambda_i &> \frac{2\bar{f}_i}{1-\varrho_i} \\ \alpha_i &> \lambda_i \frac{5\bar{f}_i\lambda_i + 4\bar{f}_i^2}{2\left(\lambda_i - 2\bar{f}_i\right)}. \end{aligned} \tag{36}$$

B. Stability for Switching Flight Modes

The problem considered in this paper, assumes that the occurrence of transitions between flight modes is determined by a switching signal $\rho(t)$. Each flight mode defines the current nonlinear closed loop system of the quadrotor. This switching signal cannot be specified a-priori because it is defined by the user of the quadrotor or depending on characteristics of the environment. So, in order to demonstrate the stability of the global nonlinear switching closed loop system, we use the common Lyapunov function principle [12]. Let us define the stability conditions with the following theorem:

Theorem 3. *Under assumptions 1, 2 and 3, the origin of the error dynamics of the closed loop system defined by (8), $U_1 - U_4$ and $\rho(t)$ is a locally asymptotically stable equilibrium point if the controller gains α_i and λi satisfy the conditions (36), regardless of the switching function $\rho(t)$.*

Proof: It is easy to see that conditions (36) assure the fulfillment of conditions (32). Then, there exists a common positive-definite Lyapunov function for each block defined as [11]:

$$V(s) = \Psi^T P \Psi \tag{37}$$

where

$$\Psi^T = \begin{bmatrix} |s|^{\frac{1}{2}} sign(s) & s \end{bmatrix}, P = \frac{1}{2}\begin{bmatrix} 4\alpha + \lambda^2 & -\lambda \\ -\lambda & 2 \end{bmatrix} \tag{38}$$

for all the flight modes considered in this work. Its derivative is obtained as

$$\dot{V}(s) = -\frac{1}{|s|^{\frac{1}{2}}}\Psi^T Q \Psi + \frac{\bar{f}}{|s|^{\frac{1}{2}}} q^T \Psi \tag{39}$$

with

$$Q = \frac{\lambda}{2}\begin{bmatrix} 2\alpha + \lambda^2 & -\lambda \\ -\lambda & -1 \end{bmatrix} \tag{40}$$

and

$$q^T = \begin{bmatrix} 2\alpha + \frac{\lambda^2}{2} & -\frac{\lambda}{2} \end{bmatrix} \tag{41}$$

which is a negative semidefinite function under conditions (36). Hence, the origin of the error dynamics of the global nonlinear switching closed-loop system is locally asymptotically stable [12]. For further details on the demonstration, please refer to [11]. ■

V. Simulation Results

In order to verify the validity and efficiency of the control proposed here, a simulation was performed. The experiment simulates a forest fire detection task, which involves several flight modes for a better user experience.

A 3D environment has been developed in simulink, also the plant was modeled according to (8) with the parameters measured from a quadrotor prototype built in the Autonomous Vehicles Laboratory (LAVAT) from Cinvestav Guadalajara, which are listed in the Table I. The solver used in the simulation is ode1(Euler) with a fixed step size of 0.001s. The gains of the controller are $\lambda_i = [10, 10, 5, 15, 15, 5]$ and $\alpha_i = [10, 10, 1, 5, 5, 1], i = 1, 3, 5, 7, 9, 11$.

TABLE I. Simulation parameters.

Parameter	*Value*	*Units*
m	1.26	Kg
d	0.23	m
I_x	5.5 x 10^{-3}	kg m^2
I_y	5.5 x 10^{-3}	kg m^2
I_z	11 x 10^{-3}	kg m^2
J	1.46 x 10^{-3}	kg m^2
b	9.4168 x 10^{-6}	N s^2/rad^2
c	2.4483 x 10^{-7}	Nm s^2/rad^2
g	9.81	m/s^2

Each flight mode can be identified by a color in the picture: yellow for autonomous control mode, blue for GPS fixed mode, and red for altitude control mode. The simulation involves five stages: 1) the UAV performs an autonomous flight mode for taking-off and following a predefined inspection trajectory, 2) a fire is detected after 32s of simulation and the UAV switches to GPS-F mode, 3) in this stage the UAV sends/saves information about the fire (position, temperature range, dimensions, etc.) and the user switches to altitude control mode, moving the quadrotor manually around the fire area, 4) once the UAV is out of risk, the user returns to GPS-F mode in order to stabilize the aircraft and be able to enter into the autonomous mode again, 5) the final stage comprise resuming the automatic inspection entire area and returns to the base. The switching between these stages occur: T1 from 1) to 2) at 32s, T2 from 2) to 3) at 38s, T3 from 3) to 4) at 42s and T4 from 4) to 5) at 45s. Also, in all the flight time the perturbations were null, except on the interval $t_{pert} = [71, 75]$s when an external wind perturbation with a speed of 3m/s in east-west direction is applied.

As we can see from the Figures 1, 2 and 3, a good trajectory tracking has been performed in the autonomous mode. Also the transitions between flight modes is achieved holding the same altitude and performing a stable flight.

It can be noted that in Figure 4 the controller for the attitude angles described in (17) is always running. Also, we can see in Figure 4 a good tracking of the desired attitude angles of

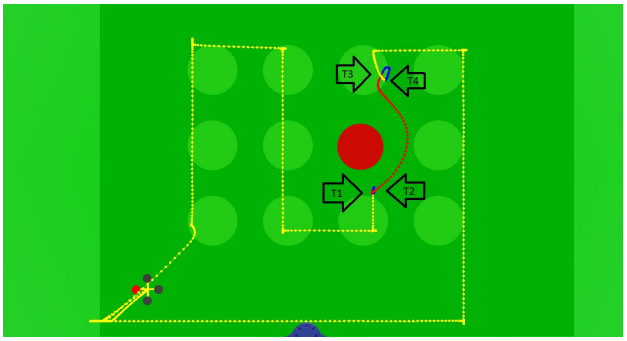

Figure 1. Aerial view of the flight performance.

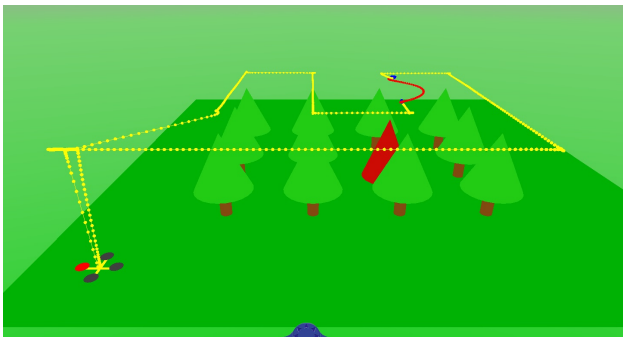

Figure 2. Lateral view of the flight performance.

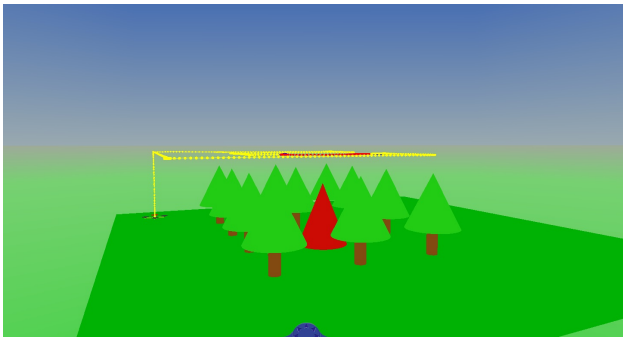

Figure 3. Lateral view of the flight performance.

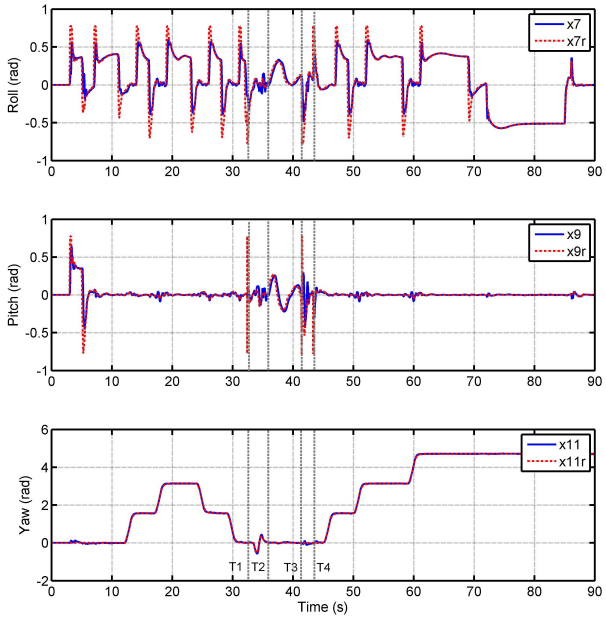

Figure 4. Quadrotor Pose.

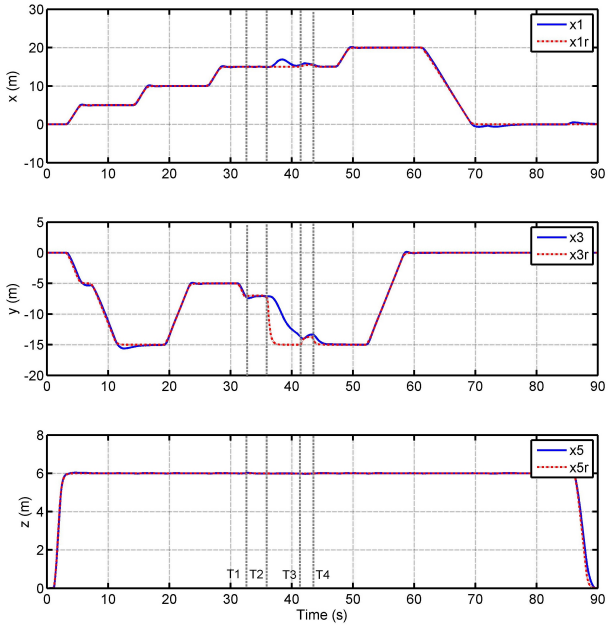

Figure 5. Quadrotor Position.

the aircraft that yields to a good tracking of the desired position for the quadrotor, as demonstrated in Figure 5. Besides, as we explained in the flight modes section, the case of study for $x-y$ position only occurs during the GPS fixed or autonomous modes, so in order to analyze the position tracking properly we need to take into account when $t = [0, 38]$ and when $t = [48, 80]$ from Figure 5.

From Figures 6 and 7 we can confirm that the forces are within the capabilities of the motors. A second order transfer function was implemented simulating the dynamics of each one of the motors in order to see if they were capable to follow the control laws. Based on the simulation results, the control compensates this unmodeled dynamic without loosing robustness, which is one of the advantages of this approach.

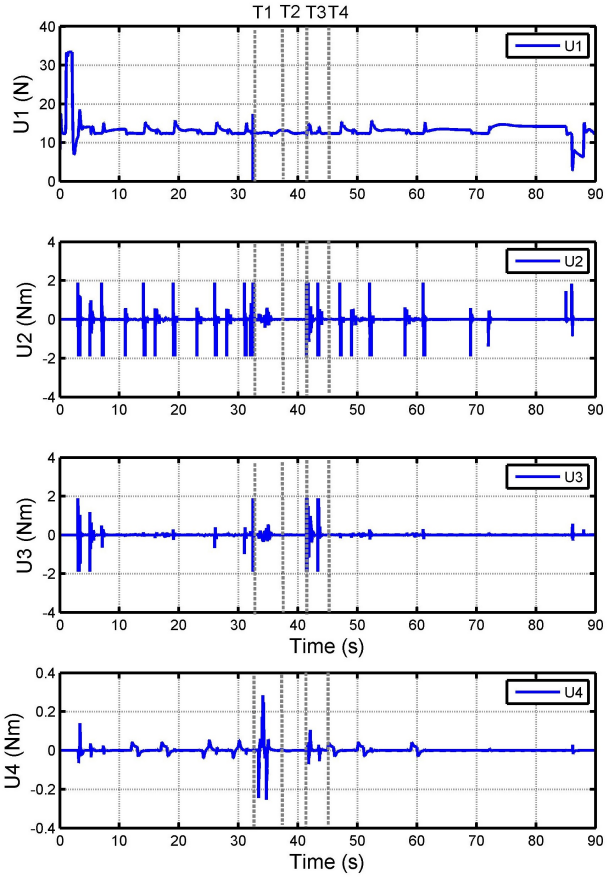

Figure 6. Control laws.

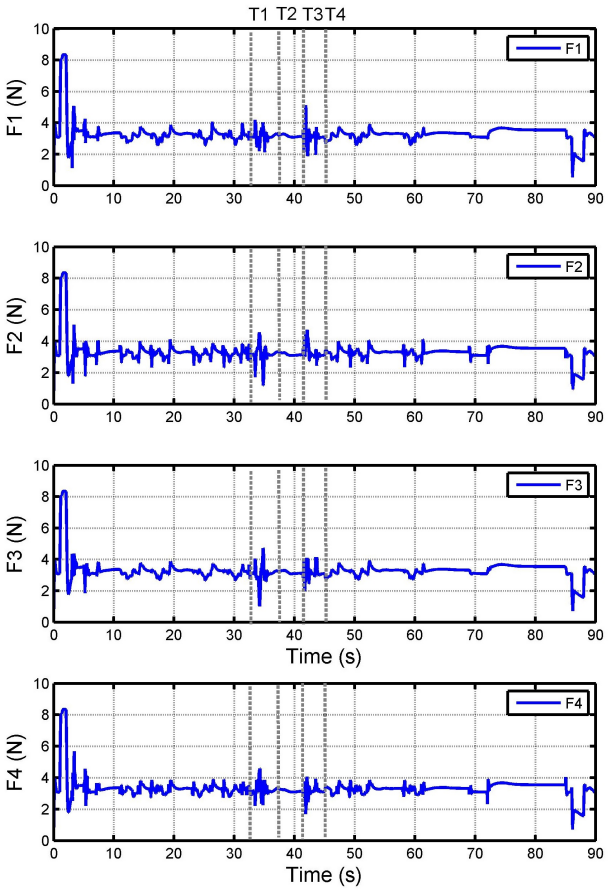

Figure 7. Forces.

VI. Conclusions

In this paper, we have proposed a framework for a multi-mode flight control system for a quadrotor based on the super twisting algorithm and the block control technique. The flight modes considered in the control scheme are manual, altitude, GPS fixed and autonomous. The control design for each flight mode is developed and the stability analysis for the closed loop system in each case were carried out. In addition, the stability for the global switched nonlinear system was demonstrated by means of the concept of a common Lyapunov function for all the flight modes.

The simulation experiment showed the performance of the proposed control scheme and it encompassed various transitions between flight modes. It can be noted that the super twisting algorithm permitted to obtain robust chattering-free control signals with a low stabilization period. This control scheme asymptotically tracks the references needed for each flight mode. Moreover, it gives the possibility to perform more complete tasks when different flight modes are required. These features are highly desired in almost every UAV application. Currently, real time implementation of the proposed control scheme is carried out at LAVAT in Cinvestav.

Acknowledgment

The authors would like to thank the National Council on Science and Technology (CONACyT) for supporting this research under grant 300573.

References

[1] L. Derafa, L. Fridman, A. Benallegue, and A. Ouldali, "Super twisting control algorithm for the four rotors helicopter attitude tracking problem," in Variable Structure Systems (VSS), 2010 11th International Workshop on, 2010, pp. 62–67. [Online]. Available: http://ieeexplore.ieee.org/stamp/stamp.jsp?arnumber=5544726

[2] A. Rabhi, M. Chadli, and C. Pegard, "Robust fuzzy control for stabilization of a quadrotor," in Advanced Robotics (ICAR), 2011 15th International Conference on, 2011, pp. 471–475. [Online]. Available: http://ieeexplore.ieee.org/stamp/stamp.jsp?arnumber=6088629

[3] H. Khebbache, B. Sait, F. Yacef, and Y. Soukkou, "Robust stabilization of a quadrotor aerial vehicle in presence of actuator faults," International Journal of Information Technology, Control and Automation, vol. 2, no. 2, 2012, pp. 1–13.

[4] A. Benallegue, A. Mokhtari, and L. Fridman, "Feedback linearization and high order sliding mode observer for a quadrotor UAV," in Variable Structure Systems, 2006. VSS'06. International Workshop on, 2006, pp. 365–372. [Online]. Available: http://ieeexplore.ieee.org/stamp/stamp.jsp?arnumber=1644545

[5] T. Madani and A. Benallegue, "Sliding mode observer and backstepping control for a quadrotor unmanned aerial vehicles," in American Control Conference, 2007. ACC '07, 2007, pp. 5887–5892. [Online]. Available: http://ieeexplore.ieee.org/stamp/stamp.jsp?arnumber=4282548

[6] S. Stevanovic, J. Kasac, and J. Stepanic, "Robust tracking control of a quadrotor helicopter without velocity measurement," in 23rd International DAAAM Symposium, Vienna, Austria, vol. 23, 2012, pp. 595–600.

[7] S. Bouabdallah, P. Murrieri, and R. Siegwart, "Design and control of an indoor micro quadrotor," in Robotics and Automation, 2004. Proceedings. ICRA'04. 2004 IEEE International Conference on, vol. 5. IEEE, 2004, pp. 4393–4398.

[8] T. Madani and A. Benallegue, "Backstepping control with exact 2-sliding mode estimation for a quadrotor unmanned aerial vehicle," in Intelligent Robots and Systems, 2007. IROS 2007. IEEE/RSJ International Conference on. IEEE, 2007, pp. 141–146.

[9] A. Levant, "Universal single-input-single-output (SISO) sliding-mode controllers with finite-time convergence," vol. 46, no. 9, 2001, pp. 1447–1451. [Online]. Available: http://ieeexplore.ieee.org/stamp/stamp.jsp?arnumber=948475

[10] J. Moreno and M. Osorio, "A Lyapunov approach to second-order sliding mode controllers and observers," in Decision and Control, 2008. CDC 2008. 47th IEEE Conference on, 2008, pp. 2856–2861. [Online]. Available: http://ieeexplore.ieee.org/stamp/stamp.jsp?arnumber=4739356

[11] L. Gonzalez-Jimenez, A. Loukianov, and E. Bayro-Corrochano, "Fully nested super-twisting algorithm for uncertain robotic manipulators," in Robotics and Automation (ICRA), 2011 IEEE International Conference on, 2011, pp. 5807–5812. [Online]. Available: http://ieeexplore.ieee.org/stamp/stamp.jsp?arnumber=5979575

[12] E. Moulay, R. Bourdaisa, and W. Perruquetti, "Stabilization of nonlinear switched systems using control lyapunov functions," Nonlinear Analysis: Hybrid Systems, vol. 1, no. 4, 2007, pp. 482–490.